Chemistry–A European Journal
Research Article
doi.org/10.1002/chem.202401645
Chemistry Europe
European Chemical Societies Publishing
www.chemeurj.org

Hot Paper

Transition Behaviors of Isostructural Hydrogen-Bonded Frameworks Composed of Naphthalene, Quinoxaline, and Pyrazinopyrazine Derivatives

Haruka Kubo,[a] Shunsuke Konishi,[b] Ryusei Oketani,[a] Takashi Hayashi,[b] and Ichiro Hisaki*[a]

A series of isostructural reticular frameworks with systematic differences on chemical structures allows us to disclose correlations between specific structural factors and properties, providing insights for designing novel porous materials. However, even slight differences in the molecular structure often lead to non-isostructural polymorphic frameworks particularly in the case of hydrogen-bonded organic frameworks (HOFs) because the structures of HOFs are based on a subtle balance of reversible interactions. In this study, we found that three simple analogues of tetracarboxylic acids with naphthalene, quinoxaline, and pyrazinopyrazine cores (**NT**, **QX**, and **PP**, respectively) yielded isostructural solvated HOFs (**NT-1**, **QX-1**, and **PP-1**, respectively), where hydrogen-bonded ***sql***-networked sheets were slip-stacked with closely similar manners. More importantly, these isostructural HOFs underwent structural transformations in different manners upon removal of the guest solvents. Comparison of the crystal structures of the HOFs before and after the transformation revealed that intermolecular interactions of the core significantly affected on rearrangements of hydrogen bonds in the transformation. The results suggest the potential to control the properties and functions of isostructural HOFs by elements in the core.

Introduction

A series of isostructural reticular frameworks with systematic differences on chemical and physical features is a suitable system for elucidating correlations between structures and properties of the materials.[1–3] Sophisticated isostructural porous frameworks possessing similar geometrical characteristics such as molecular arrangement or network topology[4–9] have been reported in metal-organic frameworks (MOFs)[10,11] and covalent organic frameworks (COFs),[12] contributing to develop the strategies for designing and modulating functionality. On the other hand, in the case of hydrogen-bonded organic frameworks (HOFs) [13–17] that have garnered attention in recent years due to its high crystallinity, structural flexibility, and reusability, attempts to construct isostructural HOFs frequently result in appearance of polymorphic frameworks. This is because HOFs are formed on the subtle balance of intermolecular interactions such as hydrogen bonds (H-bonds), π•••π interactions, and van der Waals interactions.[18] Therefore, it is more challenging to establish a design strategy of isostructural HOFs compared to other frameworks.

Recently, a handful of isostructural HOFs were successfully constructed by systematic modification of the arm moieties in building blocks (tectons).[19–21] Cao's, Chen's, and Farha's groups independently constructed isostructural pyrene-based HOFs with various aryl groups in arm moieties.[22–24] Our group also reported that hexaazatriphenylene (HAT) derivatives with different length of aryl groups as the arm moieties gave four isostructural HOFs with different pore sizes.[25,26] In these cases, robust interactions orthogonally working to the H-bonds, such as shape-fitted π-π stacking interactions of the cores, cooperatively work with directional H-bonds of the carboxy groups, giving isostructural HOFs.

In contrast, even slight differences of the core moieties may result in diverse frameworks. For example, Li and co-workers demonstrated that 1,3,5-tris(4-carboxyphenyl)benzene and its triazine analogue 2,4,6-tris(4-carboxyphenyl)triazine formed HOFs with different interpenetration manners of H-bonded honeycomb networks although the molecular shape and geometry are closely similar to each other.[27] In these cases, introduction of iminic nitrogen atoms to the core altered preferable conformation of the molecules and changed the stacking patterns in the resulting frameworks. Therefore, the approach by core-modification remains challenging to achieve isostructural HOFs, while arm-modification have been established.

To elucidate the relationship between the core and framework structure and between the core and framework properties, construction of isostructural HOFs was started using simple molecular platforms with different elements. We selected tetracarboxylic acids possessing pyrazinopyrazine, quinoxaline and naphthalene cores (**PP**, **QX**, and **NT**, respectively) as a series

[a] H. Kubo, R. Oketani, I. Hisaki
Division of Chemistry, Graduate School of Engineering Science, Osaka University, 1-3 Machikaneyama, Toyonaka, Osaka 560-8531, Japan
E-mail: i.hisaki.es@osaka-u.ac.jp
[b] S. Konishi, T. Hayashi
Department of Applied Chemistry, Graduate School of Engineering, Osaka University, 2-1 Yamadaoka, Suita, Osaka 565-0871, Japan

Supporting information for this article is available on the WWW under https://doi.org/10.1002/chem.202401645

of tectons for constructing isostructural HOFs, although HOFs of **PP** were reported in our previous work.[28]

In this study, we crystallized **QX** and **NT** and obtained their solvated HOFs **QX-1** and **NT-1**, which are isostructural with that of previously reported HOF **PP-1** formed by **PP**, where the name, **PP-1**, is used to refer the HOF instead of **CP-PP-1** used in the previous report due to easy recognition. These isostructural HOFs are formed through slip-stacking of H-bonded ***sql***-topological network layers. Interestingly, despite having almost identical geometric features like pore size and stacking manner, these isostructural HOFs undergo structural transformations in different manners by guest solvent removal (Figure 1). Single crystalline X-ray diffraction (SCXRD) analysis on the HOFs before and after the transformation revealed that intermolecular interactions of the core significantly affected on rearrangements of H-bonds on the transformation, giving frameworks **PP-2**, **QX-2**, and **NT-2** with different H-bonding motifs (Figure S1). Although dynamic behavior of porous frameworks such as MOFs have been seen in the last twenty years,[29–32] the observed transformation involving rearrangements of H-bonds are unique for HOFs. These results indicate the potential of versatile modulation of the properties and rearrangements of H-bonds in HOFs with the initial common structural characteristics through elemental altering.

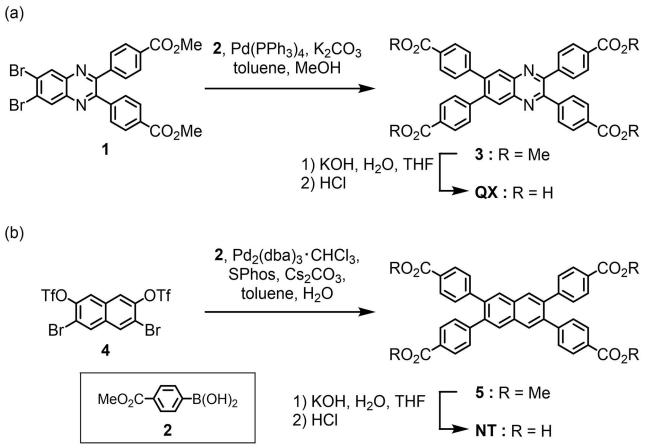

Scheme 1. Synthesis of tetracarboxylic acid building block molecules (a) **QX** and (b) **NT**.

Results and Discussion

Synthesis and Crystallization

Tetratopic tectons **QX** and **NT** were synthesized as shown in Scheme 1. Suzuki-Miyaura cross-coupling reaction of dimethyl 4,4′-(6,7-dibromoquinoxaline-2,3-diyl)dibenzoate (**1**)[33] and (4-(methoxycarbonyl)phenyl)boronic acid (**2**) gave ester precursor **3**. Hydrolysis of **3** in the presence of KOH yielded tetracarboxylic acid **QX**.[34] Similarly, Suzuki-Miyaura cross-coupling reaction of 3,6-dibromonaphthalene-2,7-diyl bis(trifluoromethanesulfonate) (**4**), which was synthesized according to the literature,[35] and **2**

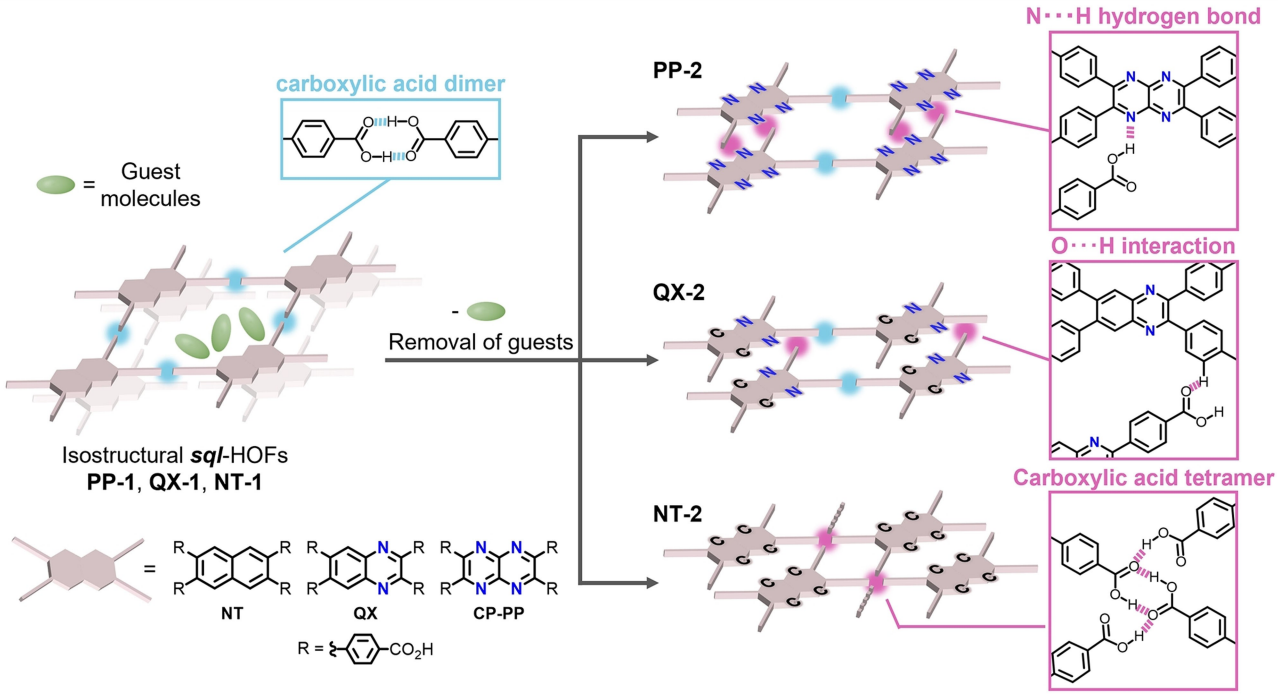

Figure 1. Overview of this study: Transformations of isostructural ***sql***-topological hydrogen-bonded organic frameworks (HOFs) composed of pyrazinopyrazine-, quinoxaline-, and naphthalene-based tetracarboxylic acids **PP**, **QX**, and **NT**, respectively.

gave ester precursor **5**, which was subsequently hydrolyzed to yield **NT**. Tectons **QX** and **NT** were characterized by ^{1}H and ^{13}C NMR spectroscopy and HR-MS. Crystallization of **QX** and **NT** was conducted by slow evaporation of a mixed solution of *N,N*-dimethylformamide (DMF) and *o*-dichlorobenzene (*o*-DCB) at 75 °C to yield solvated HOFs **QX-1** and **NT-1** as yellow plate crystals and colorless block crystals, respectively. These single crystals were subjected to SCXRD analysis.

Crystal Structures of the Initial Solvated HOFs

Figure 2 shows overviewed crystal structures of **QX-1** and **NT-1**, together with that of previously reported **PP-1**[28] as a reference. In these crystals, the tetracarboxylic acids are connected through intermolecular H-bonds, giving a ***sql***-topological two-dimensional (2D) sheet. The sheets are assembled with a slip-stacking fashion to give the isostructural frameworks, although relative orientation of the neighboring sheets slightly differs from each other. The details of these crystal structure are discussed as follows.

Detailed crystal structures of **QX-1** and **NT-1** are shown in Figure 3. **QX-1** belongs to the triclinic system with space group *P*-1. Since the quinoxaline core of **QX** is disordered in the crystal, the molecule has an inversion center at the center of the core: The atoms at positions 1, 4, 5, and 8 of the quinoxaline moiety were refined with sp^2-carbon and nitrogen atoms sharing position at a 50% occupancy each (Figure 3a). The twisted angles between the two independent phenylene groups and the quinoxaline core are 42.7° and 47.4°. The peripheral carboxy groups of **QX** form a dimer through the self-complementary H-bond with a O•••O distance of 2.60–2.61 Å to give a ***sql***-topological 2D networked sheet. The sheet contains rhombic voids with aperture dimension of 27.1 Å×11.1 Å (Figure 3b). The sheets are stacked in an inclined AA pattern along the *a* axis with an interplanar distance of 3.74 Å. C–H•••π interaction are formed between the aromatic hydrogen atom of the phenylene group and the benzene ring of **QX** or the phenylene group in adjacent layer (Figure S3). Additionally, weak H-bonding interactions such as C–H•••N and C–H•••O interactions were also observed. C–H•••N interactions are formed between the nitrogen atom of **QX** and the aromatic hydrogen atom of the phenylene group with the C–H•••N distance of 2.72 Å. C–H•••O interactions are formed between the O atom of carboxylic acid and the aromatic hydrogen atom of the phenylene group in adjacent layer with the C–H•••O distance of 2.58 Å. HOF **QX-1** has inclusion channels with rectangular-shaped aperture with 8.34 Å×7.94 Å (Figure 3c). A void ratio was estimated to be 30.3% by PLATON.[36] The guest molecules were severely disordered, making it difficult to determine their positions in **QX-1** (Figure S2).

NT-1 also belongs to the triclinic system with space group *P*-1. The twisted angles between the two independent phenylene groups and the quinoxaline core are 49.5° and 50.4° (Figure 3d). The peripheral carboxy groups formed a dimer through the self-complementary H-bond with a O•••O distance of 2.60–2.63 Å to give a ***sql***-topological 2D networked sheet. The sheet contains rhombic voids with aperture dimensions of 25.6 Å×11.8 Å (Figure 3e). The sheets are stacked in an inclined AA pattern along the *a* axis with an interplanar distance of 4.42 Å. C–H•••π interaction are formed between the aromatic hydrogen atom of the phenylene group and benzene ring of **NT** or the phenylene group in adjacent layer (Figure S5). C–H•••O interactions are also formed between the O atom of carboxylic acid and the aromatic hydrogen atom of the phenylene group in adjacent layer with the C–H•••O distance of 2.56–2.61 Å. The HOF has two types of inclusion channels with rectangular-shaped aperture with 8.71 Å×8.21 Å and 9.53 Å×8.92 Å, respectively (Figure 3f). A void ratio was estimated to be 30.1% by PLATON. Although guest molecules were disordered, the alignment of a part of guest molecules could be determined. The *o*-DCB was inclined at 73.09° to the naphthalene core, forming a C–H•••π interaction.

There are several subtle differences among **PP-1**, **QX-1**, and **NT-1** in terms of molecular geometry and distortions of the ***sql***-topological layer although they have common slip-stacked layered structures (Table 1). The dihedral angles between the phenylene groups and the core (ω) are 19.7° and 55.9° for **PP**, whereas 42.4° and 47.4° for **QX**, and *ca.* 50° for **NT**. The steric hindrance of the aromatic hydrogen atoms in the core of **QX** or **NT** prevent the dihedral angle from being small. This tendency is also observed in other ***sql***-topological HOFs composed of X-

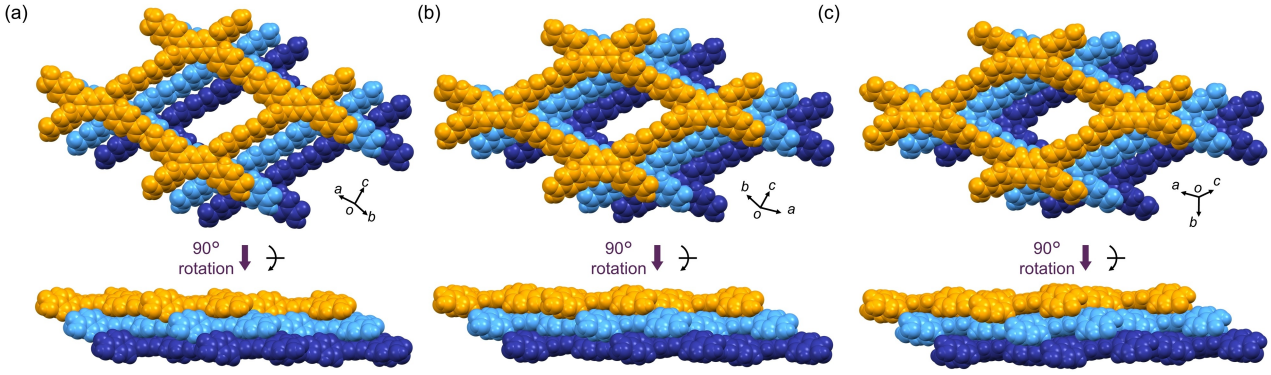

Figure 2. Overviewed crystal structures of isostructural three HOFs (a) **PP-1**, (b) **QX-1**, and (c) **NT-1**. The structure of **PP-1** was drawn using crystal data (CCDC No. 2078212) previously reported.[28]

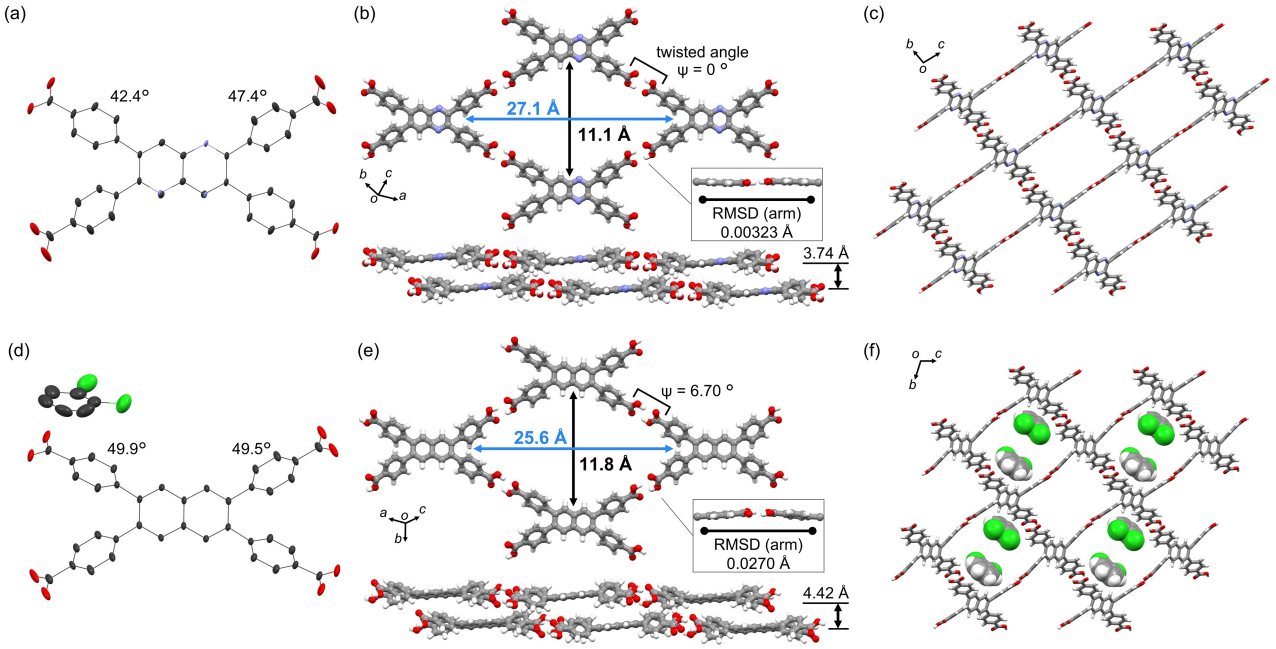

Figure 3. Crystal structures of (a–c) **QX-1** and (d–f) **NT-1**. (a, d) Molecular structure of (a) **QX** and (d) **NT** and *o*-DCB drawn with anisotropic displacement ellipsoids with 50% probability. (b, e) H-bonded ***sql***-topological sheet composed of four molecules viewed from above (top) and two stacked sheets viewed from side (bottom) in (b) **QX-1** and (e) **NT-1**. (c, f) Packing diagrams viewed from the *a* axis. The *o*-DCB molecules are included in voids, although they are not shown in the figure due to disorder in (c) **QX-1**. A part of guest molecules were capable of solving as shown in (f) **NT-1**. The atoms at positions 1, 4, 5, and 8 of the quinoxaline moiety were refined with sp^2-carbon and nitrogen atoms sharing position at a 50% occupancy each, and one of sp^2-carbon and nitrogen atoms is omitted for clarity in (b) and (c).

Table 1. Selected structural parameters of three HOFs **PP-1**, **QX-1**, and **NT-1**.

	PP-1	QX-1	NT-1
ω[a]/	19.7, 55.9	42.4, 47.4	47.7, 50.4, 49.5, 49.9
Dimension of rhombic aperture/Å	13.7×24.5	11.1×27.1	11.8×25.6
O•••O distance of the carboxylic acid dimer/Å	2.62	2.60–2.61	2.60–2.63
Stacking distance/Å	3.36	3.74	4.42
Void ratio[b]	29.9%	30.3%	30.1%
ψ[c]/°	0	0	5.47, 8.44 (avg. 6.70)
RMSD (arm)[d]/Å	0.00175	0.00323	0.0270

[a] The dihedral angles of carboxyphenyl groups against the central core. [b] Solvent accessible surface. [c] The dihedral angles between H-bonded carboxyphenyl groups. [d] The root mean square deviation (RMSD) on the planes formed by H-bonded carboxyphenyl groups.

shaped tetracarboxylic acids: for example, tetrakis(carboxyphenyl)benzene derivative **X-Ph**[37] exhibits the ω values of 51.1° and 52.7° in the HOF, while **X-TTF**[37,38] and **Br-PQ**[39] exhibits smaller values [35.1° and 43.8° for **X-TTF**, and 21.8° and 63.4° for **Br-PQ**] due to lack of the aromatic hydrogen atoms at the ortho positions in the core.

The bending of carboxylic acid dimers is observed only in **NT-1**, resulting slightly distorted rhombic network. The twist angle of the carboxylic acid dimers (ψ) is 6.7° for **NT-1** while the carboxylic acid dimers are not twisted at all in **PP-1** and **QX-1**. To evaluate distortions of the rhombic frameworks, we calculated the root mean square deviation (RMSD) on the planes formed by H-bonded carboxyphenyl groups [RMSD(arm)]. The RMSD(arm) for **NT-1** is approximately ten times larger than that for **PP-1** and **QX-1**, indicating that **NT-1** is more distorted framework compared to the other two.

Structural Transformations

In the thermogravimetric (TG) and differential thermal (DT) analyses, it was observed that **PP-1**, **QX-1**, and **NT-1** showed each total weight loss of 42%, 37% and 38%, respectively, which corresponds to a host-guest ratio of 1:2 (Figure 4a–c). The TG curve of **PP-1** indicates *o*-DCB molecules are released in three steps. Similarly, the TG curve of **QX-1** indicates that *o*-DCB molecules are clearly released in two steps. Three-fourths of *o*-DCB molecules are released in the first step up to 156 °C. The

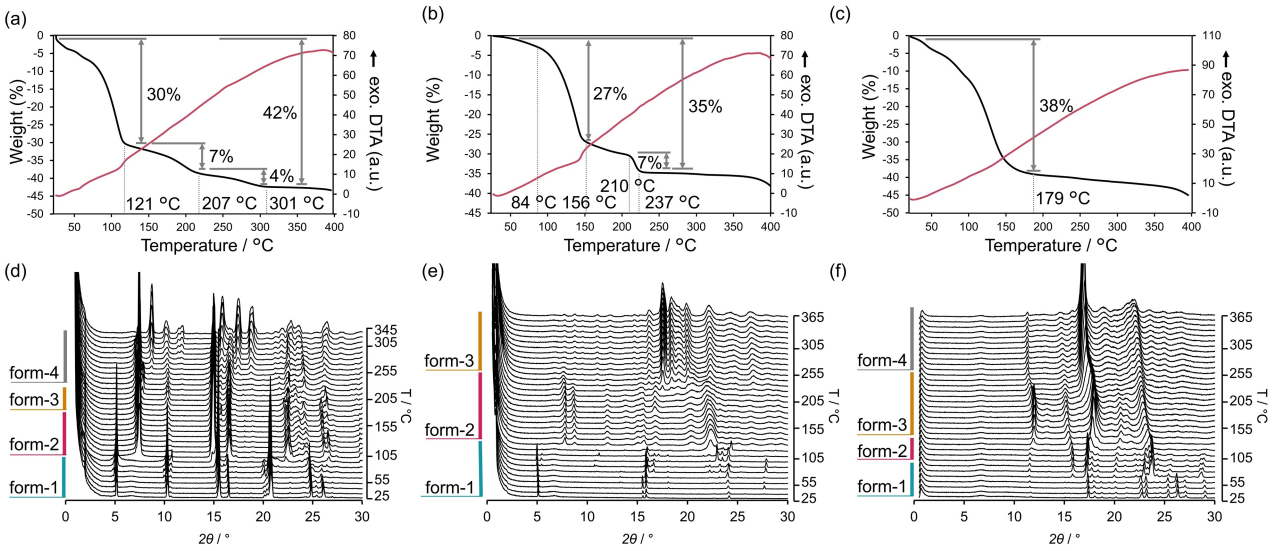

Figure 4. Thermal behaviors of (a, d) **PP-1**, (b, e) **QX-1**, and (c, f) **NT-1**. (a–c) TG-DT curves and (d–f) VT-PXRD patterns.

other *o*-DCB molecules are released in the second step up to 210 °C. In contrast, the TG curve of **NT-1** has no clear plateau under 179 °C, suggesting continuous release of the solvent. Molecules of *o*-DCB began to desorb gradually at room temperature and completed desorption at 179 °C. These behaviors are strongly related to disorder of *o*-DCB molecules in the crystal structures shown in Figure 3. In all cases of **PP-1**, **QX-1**, and **NT-1**, additional heating resulted in weight loss beyond 400 °C, corresponding the onset of decomposition.

To investigate their transition behaviors triggered by removal of solvent molecules, variable-temperature powder X-ray diffraction (VT-PXRD) patterns were recorded on as-formed crystalline bulks of solvated HOFs as heated from room temperature to 365 °C (Figures 4d–f and S7–S9). **PP-1** underwent three-step structural transformations including the first transformation from **PP-1** to **PP-2** at 105 °C followed by continuous structural changes, which is the similar behavior with those reported previously.[28] **QX-1** transformed to **QX-3** via **QX-2** through two-step structural changes upon heating. The peak at $2\theta = 5.1°$ disappeared at 125 °C, and new peaks appeared at $2\theta = 7.8°$ and 8.8°, indicating that **QX-1** transformed to **QX-2**. Further heating up to 225 °C led to the diminution of these peaks, and a new peak at $2\theta = 11.1°$ appeared, implying that **QX-2** transformed to **QX-3**. In the case of **NT-1**, the initial form seems to transform to **NT-4** by three steps via **NT-2** and **NT-3**. The changes, however, occurred gradually, which obviously differs from non-continuous stepped changes observed for **QX-1**. Transformation of **NT-1** into **NT-2** took place at a lower temperature of 65 °C compared to **QX-1**. Subsequently, in the temperature range of 115 °C–235 °C, a gradual shift towards lower angles was observed for $2\theta = 11.8$ and 17.7°, indicating a continuous structural change (**NT-3**). At 245 °C, the peak at $2\theta = 11.8°$ no longer shifted, corresponding the transition to **NT-4**. This result suggests that **PP-1** and **NT-1** exhibited similar transition behaviors, while **QX-1** transformed less readily compared to the former two, presumably due to less uniformity of the crystal provided by disorder of the quinoxaline core as well as that of the included solvent molecules. To evaluate reversibility of these transformations, **QX-3** and **NT-3** were immersed in *o*-DCB. Their PXRD patterns after immersion showed that they lost crystallinity (Figures S10 and S11).

To elucidate transformed structures, we attempted to obtain single crystals of their intermediate forms. After many efforts, we revealed that placing **QX-1** and **NT-1** under reduced pressure overnight each at 60 °C and at room temperature, respectively, yielding the corresponding crystals **QX-2** and **NT-2**, that partially maintain single crystallinity suitable for SCXRD analysis, although quality of crystal data of **QX-2** remains low despite our efforts. Their overviewed crystal structures are shown in Figure 5. The crystal structure of **PP-2** was drawn on the basis of reported one.[28] In all cases of **PP-1**, **QX-1**, and **NT-1**, the two diagonal carboxy groups retained the H-bonded dimers, while the other two dimers were cleaved, resulting in different alignments of one-dimensional (1D) chain motifs.

In the case of **PP-2**, the 1D chains interact through hetero H-bonds between the carboxy group and the nitrogen atom of the **PP** core as reported.[28] In the case of **QX-2**, 1D chain of **QX** formed by H-bonding of carboxylic acid dimers with an O•••O distance of 2.63 Å are stacked in the *c*-axis direction, through π-π and C–H•••π interactions between the core and peripheral phenyl groups, resulting in a layered structure with interlayer distance of 3.62 Å (Figure 6a). On the other hand, there is no significant interactions between the 1D chains adjacent in the same plane. Only weak interactions between the carboxy oxygen atom and aromatic hydrogen atoms are suggested. Disordered solvent molecules may also support this packing structure. The twist angles between the peripheral phenyl groups and the core plane are 28.6° and 60.8°, which are smaller than the dimer formation angles of the carboxylic phenyl groups in **QX-1** (42.7° and 47.4°). The sheet contains

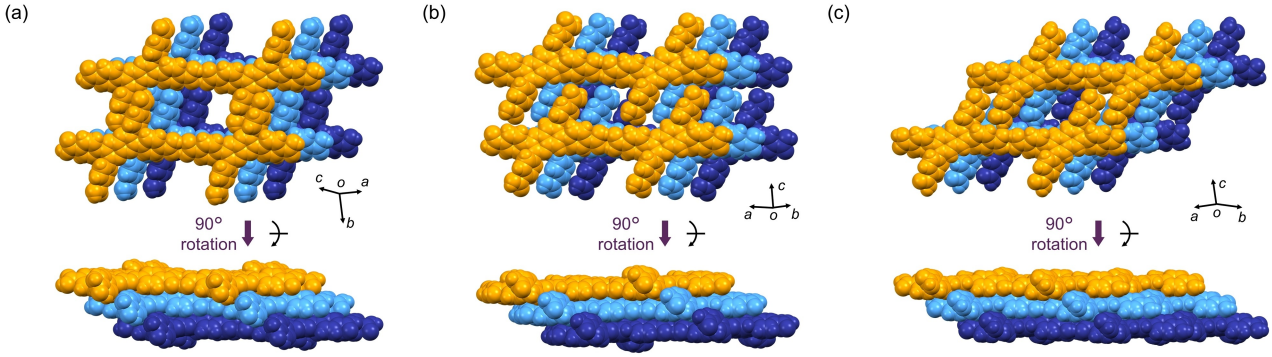

Figure 5. Overviews of three transformed HOFs (a) **PP-2**, (b) **QX-2**, and (c) **NT-2**. The structure of **PP-2** was drawn using crystal data (CCDC No. 2080627) previously reported.[28]

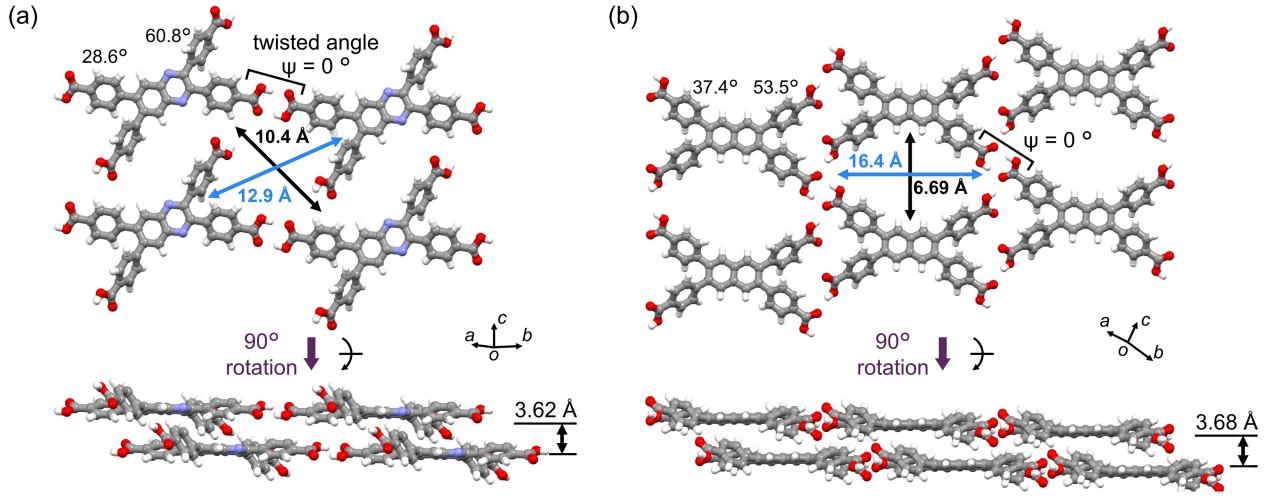

Figure 6. (a) H-bonded 1D chain motifs viewed from above (top) and two layers of sheets viewed from side (bottom) in **QX-2**. The atoms at positions 1, 4, 5, and 8 of the quinoxaline rings were refined with sp^2-carbon and nitrogen atoms sharing position at a 50% occupancy each. One of sp^2-carbon and nitrogen atoms is omitted for clarity in (a). (b) H-bonded 2D chain network motif viewed from above (top) and two layers of sheets viewed from side (bottom) in **NT-2**. The *o*-DCB are included in voids, although they are not shown in the figure due to disorder in both of (a) **QX-2** and in (b) **NT-2**.

rhombic voids with aperture dimension of 16.2 Å×12.9 Å. The void ratio was estimated to be 8.2%. The adjacent layers are overlapped due to π-π stacking interactions between the phenylene group and carboxylic group (Figure S4).

NT formed cross-shaped carboxylic acid tetramer by combination of the carboxylic acid dimer and other two carboxy groups (Figure 6b). This H-bonding motif is also observed in other HOFs, such as **PFC-79**[38] based on a tetrathiafulvalene tetracarboxylic acid derivative and, **BrPQ-2**[39] based on a dibromopyrazinoquinoxaline tetracarboxylic acid derivative. The O•••O distance of the carboxyl dimers is 2.64 Å, and that in the branched H-bonds is 2.67 Å. Similar to **QX-2**, stacking was achieved through π•••π interactions between the core and peripheral phenyl groups or C–H•••π interactions, resulting in a layered structure with interlayer distance of 3.68 Å. The twist angles of the peripheral phenyl groups to the core plane are 37.4° and 53.5°, smaller than the dimer formation angles of the carboxylic phenyl groups in **NT-1** (49.5° and 50.4°). The sheet has a rhombic void with small aperture dimension of 16.4 Å×6.69 Å. The void ratio was estimated to be 5.7%. The adjacent layers are overlapped due to π-π stacking interactions between the phenylene group and carboxylic group (Figure S6). The host-guest ratios in both **QX-2** and **NT-2** were 1:1, identified by ^{1}H NMR of the crystals (Figure S23), while the position of guest molecules couldn't be determined by SCXRD because of their severe disorder.

H-bonding interactions between the 1D chain motifs were calculated. In the case of **PP-2**, hetero H-bonds between the carboxy group and nitrogen atom in the **PP** cores are estimated to be −51.3 kJ/mol (Figure S12 and Tables S2–S6). A weak C–H•••O H-bond between the carbonyl and phenylene groups in **PP-2** has a binding energy of −10.9 kJ/mol. In the case of **QX-2**, only C–H•••O interactions were observed between the carbonyl and phenylene groups with an interaction energy of −12.0 kJ/mol (Figure S13 and Tables S7–S10). A blanched H-bond observed in **NT-2** exhibits an interaction energy of 38.5 kJ/mol (Figure S14 and Tables S11–S13). Thus, H-bonds

working between the 1D chain motifs are larger in the order of **QX-2**, **NT-2**, and **PP-2**.

Compared to PXRD patterns simulated from crystal structures, PXRD patterns of **QX-2** observed at 125 °C match simulated patterns although observed patterns included other peaks. Through this comparison, the crystalline bulk of **QX-2** seemed to contain several polymorphic crystal structures. Solving the crystal structure using a PXRD pattern of **NT-2** was hard because intensity of PXRD peaks in the small angle region was too weak for indexing. However, we obtained the crystal structure of one of the phases undergoing continuous change by SCXRD. Attempts were also made to reveal crystal structures of **QX-3**, **NT-3**, and **NT-4** by SCXRD analyses on solid samples obtained by further heating, resulting failure due to significant decrease in crystallinity. However, the solvent free forms **QX-3** and **NT-3** showed permanent porosity with small Brunauer-Emmett-Teller (BET) surface areas of 49 $m^2 g^{-1}$ and 288 $m^2 g^{-1}$, respectively (Figures S15–S18).

Conclusions

We constructed novel HOFs, **QX-1** and **NT-1**, consisting of tetracarboxylic acids with quinoxaline and naphthalene core, and explored the structures and transition behaviors of three isostructural HOFs **PP-1**, **QX-1**, and **NT-1** to elucidate the effects of the nitrogen atoms in the core. SCXRD analysis revealed that the frameworks of the three HOFs were geometrically similar, *i.e.* isostructures. Their thermal behaviors showed that **PP-1**, **QX-1** and **NT-1** underwent structural transitions into **PP-2**, **QX-2** and **NT-2**, respectively, upon removal of guest molecules, trigered by reconstruction of intermolecular H-bonds. **PP-2** contains hetero H-bonds between iminic nitrogen and carboxylic hydrogen. **QX-2** contains weak C–H•••O interactions. **NT-2** contains blanched H-bonds of carboxylic acid tetramers. The presence of iminic nitrogen atoms in the core provided stabilization through N•••H H-bond formation, while the sp^2-carbon atoms participated in weak CH•••π interactions. These results contribute to establishing guidelines for controlling transition behavior without altering the initial framework structure.

Supporting Information

The authors have cited additional references within the Supporting Information (Refs. [40–50]). Crystal structures of **QX-1** (CCDC 2350221), **NT-1** (CCDC 2350222), **QX-2** (CCDC 2350223), and **NT-2** (CCDC 2350224). These data are provided free of charge by the joint Cambridge Crystallographic Data Centre and Fachinformationszentrum Karlsruhe Access Structures service.

Acknowledgements

This work was supported by KAKENHI (JP21H01919, JP22H05461, JP23H04029, and JP24K01468) from JSPS and MEXT Japan. H. K. thanks finantial support by JST, the establishment of university fellowships towards the creation of science technology innovation (JPMJFS2125). I. H. thanks Hoansha Foundation and the Multidisciplinary Research Laboratory System for Future Developments (MRL), Graduate School of Engineering Science, Osaka University for their finantial support. The authors thank the Cybermedia Center, Osaka University, for use of the Super-computer for Quest to Unsolved Interdisciplinary Datascience (SQUID). The authors acknowledge Prof. Dr. N. Tohnai and Ms. M. Naruoka at Osaka University for gas sorption experiments and Ms. R. Miyake at Osaka University for HR-MS analysis.

Conflict of Interests

The authors declare no conflict of interest.

Data Availability Statement

The data that support the findings of this study are available inthe supplementary material of this article.

Keywords: Hydrogen-bonded framework · Isostructure · Flexibility · Porous molecular crystal · Crystal engineering

[1] H. Deng, C. J. Doonan, H. Furukawa, R. B. Ferreira, J. Towne, C. B. Knobler, B. Wang, O. M. Yaghi, *Science* **2010**, *327*, 846–850.
[2] L. Feng, K. Y. Wang, G. S. Day, H. C. Zhou, *Chem. Soc. Rev.* **2019**, *48*, 4823–4853.
[3] C. S. Diercks, O. M. Yaghi, *Science* **2017**, *355*, aal1585.
[4] A. G. Slater, A. I. Cooper, *Science* **2015**, *348*, aaa8075.
[5] C. S. Diercks, Y. Liu, K. E. Cordova, O. M. Yaghi, *Nat. Mater.* **2018**, *17*, 301–307.
[6] M. J. Kalmutzki, N. Hanikel, O. M. Yaghi, *Sci. Adv.* **2018**, *4*, eaat9180.
[7] C. Gropp, S. Canossa, S. Wuttke, F. Gándara, Q. Li, L. Gagliardi, O. M. Yaghi, *ACS Cent. Sci.* **2020**, *6*, 1255–1273.
[8] Y. B. Zhang, Q. Li, H. Deng, *Nano Res.* **2021**, *14*, 335–337.
[9] W. Xu, B. Tu, Q. Liu, Y. Shu, C. C. Liang, C. S. Diercks, O. M. Yaghi, Y. B. Zhang, H. Deng, Q. Li, *Nat. Rev. Mater.* **2020**, *5*, 764–779.
[10] O. M. Yaghi, G. Li, H. Li, *Nature* **1995**, *378*, 703–706.
[11] M. Kondo, T. Yoshitomi, K. Seki, H. Matsuzaka, S. Kitagawa, *Angew. Chem. Int. Ed.* **1997**, *36*, 1725–1727.
[12] A. P. Côté, A. I. Benin, N. W. Ockwig, M. O'Keeffe, A. J. Matzger, O. M. Yaghi, *Science* **2005**, *310*, 1164–1166.
[13] K. Endo, T. Sawaki, M. Koyanagi, K. Kobayashi, Y. Aoyama, K. Endo, Y. Aoyama, H. Masuda, *J. Am. Chem. Soc.* **1995**, *117*, 8341–8352.
[14] P. Sozzani, A. Comotti, R. Simonutti, T. Meersmann, J. W. Logan, A. Pines, *Angew. Chem. Int. Ed.* **2000**, *39*, 2695–2699.
[15] Y. He, S. Xiang, B. Chen, *J. Am. Chem. Soc.* **2011**, *133*, 14570–14573.
[16] I. Hisaki, C. Xin, K. Takahashi, T. Nakamura, *Angew. Chem. Int. Ed.* **2019**, *58*, 11160–11170.
[17] R. B. Lin, Y. He, P. Li, H. Wang, W. Zhou, B. Chen, *Chem. Soc. Rev.* **2019**, *48*, 1362–1389.
[18] H. Wang, Z. Bao, H. Wu, R. B. Lin, W. Zhou, T. L. Hu, B. Li, J. C. G. Zhao, B. Chen, *Chem. Commun.* **2017**, *53*, 11150–11153.
[19] A. Pulido, L. Chen, T. Kaczorowski, D. Holden, M. A. Little, S. Y. Chong, B. J. Slater, D. P. McMahon, B. Bonillo, C. J. Stackhouse, A. Stephenson,

C. M. Kane, R. Clowes, T. Hasell, A. I. Cooper, G. M. Day, *Nature* **2017**, *543*, 657–664.
[20] M. I. Hashim, H. T. M. Le, T. H. Chen, Y. S. Chen, O. Daugulis, C. W. Hsu, A. J. Jacobson, W. Kaveevivitchai, X. Liang, T. Makarenko, O. Miljanić, I. Popovs, H. V. Tran, X. Wang, C. H. Wu, J. I. Wu, *J. Am. Chem. Soc.* **2018**, *140*, 6014–6026.
[21] X. Ding, Z. Liu, Y. Zhang, G. Ye, J. Jia, J. Chen, *Angew. Chem. Int. Ed.* **2022**, *61*, e202116483.
[22] Q. Yin, P. Zhao, R. J. Sa, G.-C. Chen, J. Lü, T. F. Liu, R. Cao, *Angew. Chem.* **2018**, *130*, 7817–7822.
[23] B. Wang, X. L. Lv, J. Lv, L. Ma, R. B. Lin, H. Cui, J. Zhang, Z. Zhang, S. Xiang, B. Chen, *Chem. Commun.* **2019**, *56*, 66–69.
[24] Y. Wang, K. Ma, J. Bai, T. Xu, W. Han, C. Wang, Z. Chen, K. O. Kirlikovali, P. Li, J. Xiao, O. K. Farha, *Angew. Chem. Int. Ed.* **2022**, *61*, e202115956.
[25] Y. Suzuki, M. Gutiérrez, S. Tanaka, E. Gomez, N. Tohnai, N. Yasuda, N. Matubayasi, A. Douhal, I. Hisaki, *Chem. Sci.* **2021**, *12*, 9607–9618.
[26] Y. Suzuki, M. Yamaguchi, R. Oketani, I. Hisaki, *Mater. Chem. Front.* **2022**, *7*, 106–116.
[27] Y. L. Li, E. V. Alexandrov, Q. Yin, L. Li, Z. Bin Fang, W. Yuan, D. M. Proserpio, T. F. Liu, *J. Am. Chem. Soc.* **2020**, *142*, 7218–7224.
[28] Q. Ji, K. Takahashi, S. I. Noro, Y. Ishigaki, K. Kokado, T. Nakamura, I. Hisaki, *Cryst. Growth Des.* **2021**, *21*, 4656–4664.
[29] R. Kitaura, K. Seki, G. Akiyama, S. Kitagawa, *Angew. Chem. Int. Ed.* **2003**, *42*, 428–431.
[30] S. Horike, S. Shimomura, S. Kitagawa, *Nat. Chem.* **2009**, *1*, 695–704.
[31] C. Zhao, C. S. Diercks, C. Zhu, N. Hanikel, X. Pei, O. M. Yaghi, *J. Am. Chem. Soc.* **2018**, *140*, 16438–16441.
[32] X. Liu, J. Li, B. Gui, G. Lin, Q. Fu, S. Yin, X. Liu, J. Sun, C. Wang, *J. Am. Chem. Soc.* **2021**, *143*, 2123–2129.
[33] A. V. Yagodin, I. A. Mikheev, D. A. Bunin, A. A. Sinelshchikova, A. G. Martynov, Y. G. Gorbunova, A. Y. Tsivadze, *Dyes Pigm.* **2023**, *216*, 111326. .
[34] S. Mi, L. Wang, H. Guo, Y. Su, S. Wang, J. Xu, J. Cao, X. Guo, *Cryst. Growth Des.* **2024**, *24*, 405–413.
[35] Y. Li, X. Su, W. Zheng, J. J. Zheng, L. Guo, M. Bonn, X. Gao, H. I. Wang, L. Chen, *Angew. Chem. Int. Ed.* **2023**, *62*, e202216795..
[36] A. L. Spek, *Acta Cryst. D: Biol. Crystallogr.* **2009**, *65*, 148–155..
[37] I. Hisaki, N. Q. Emilya Affendy, N. Tohnai, *CrystEngComm* **2017**, *19*, 4892–4898.
[38] X. Y. Gao, Y. L. Li, T. F. Liu, X. S. Huang, R. Cao, *CrystEngComm* **2021**, *23*, 4743–4747.
[39] H. Kubo, R. Oketani, I. Hisaki, *Chem. Commun.* **2021**, *57*, 8568–8571.

Manuscript received: April 26, 2024
Accepted manuscript online: June 4, 2024
Version of record online: July 16, 2024